Toxicology in Vitro 27 (2013) 1762–1770

Contents lists available at SciVerse ScienceDirect

Toxicology in Vitro

journal homepage: www.elsevier.com/locate/toxinvit

$PM_{2.5}$-induced oxidative stress triggers autophagy in human lung epithelial A549 cells

Xiaobei Deng [a], Fang Zhang [a], Wei Rui [a], Fang Long [a], Lijuan Wang [b], Zhaohan Feng [c,*], Deliang Chen [a], Wenjun Ding [a,*]

[a] Laboratory of Environment and Health, College of Life Sciences, University of Chinese Academy of Sciences, No. 19A Yuquan Road, Beijing 100049, China
[b] Institute of Zoology, Chinese Academy of Sciences, Beichen Xi Road 1-5, Beijing 100101, China
[c] Department of Urology, China–Japan Friendship Hospital, Beijing 100029, China

ARTICLE INFO

Article history:
Received 22 November 2012
Accepted 7 May 2013
Available online 17 May 2013

Keywords:
$PM_{2.5}$
Oxidative stress
Autophagy
Lung epithelial A549 cells

ABSTRACT

Exposure to higher levels of air pollution particulate matter (PM) with an aerodynamic diameter of less than 2.5 μm ($PM_{2.5}$) links with an increased risk of cardiovascular and respiratory deaths and hospital admission as well as lung cancer. Although the mechanism underlying the correlation between $PM_{2.5}$ exposure and adverse effects has not fully elucidated, $PM_{2.5}$-induced oxidative stress has been considered as an important molecular mechanism of $PM_{2.5}$-mediated toxicity. In this work, human lung epithelial A549 cells were used to further investigate the biological effects of $PM_{2.5}$ on autophagy. The cell viability showed both time- and concentration-dependent decrease when exposure to $PM_{2.5}$, which can be attributed to increase of the levels of extracellular lactate dehydrogenase (LDH) release and intracellular reactive oxygen species (ROS) generation in A549 cells. Moreover, $PM_{2.5}$-induced oxidative damage in A549 cells was observed through the alteration of superoxide dismutase (SOD) and catalase (CAT) activities compared to the unexposed control cells. $PM_{2.5}$-induced autophagy was indicated by an increase in microtubule-associated protein light chain-3 (LC3) puncta, and accumulation of LC3 in both time- and concentration-dependent manner. $PM_{2.5}$-induced mRNA expression of autophagy-related protein Atg5 and Beclin1 was also observed compared with those of the unexposed control cells. These results suggest the possibility that $PM_{2.5}$-induced oxidative stress probably plays a key role in autophagy in A549 cells, which may contribute to $PM_{2.5}$-induced impairment of pulmonary function.

1. Introduction

Epidemiological studies have demonstrated that long-term exposure to high concentrations of airborne particulate matter (PM) increases the risk of respiratory diseases, including lung cancer and atherosclerosis (Pope et al., 2002; Knaapen et al., 2004). Among them, chronic respiratory diseases are one of the major problems concerning public health subjects. Generally, the adverse effect of PM on human health is determined by its size, surface area, and chemical composition of the PM. In particular, increased exposure to the fine particles with a mean aerodynamic diameter of <2.5 μm ($PM_{2.5}$) is associated with an increased risk of cardiovascular and respiratory deaths (Anderson et al., 2012; Ghio et al., 2012). $PM_{2.5}$ has been listed as an important air pollutant due to its potential to bioaccumulation and oxidative damage to humans (Brunekreef and Holgate, 2002).

$PM_{2.5}$-induced oxidative stress has been considered as an important molecular mechanism of $PM_{2.5}$-mediated toxicity. Oxidative stress refers to a critical imbalance between the production of reactive oxygen species (ROS) and antioxidant defenses (Brigelius-Flohé, 2009), and ROS has been identified as signaling molecules in various pathways regulating both cell survival and cell death (Azad et al., 2009; Wu, 2006). $PM_{2.5}$-induced ROS directly interacts with antioxidant enzymes, such as superoxide dismutase (SOD), glutathione peroxidase (GPx) and catalase (CAT), causing lost of enzymatic activity *in vivo* and *in vitro* (Chirino et al., 2010; Pamplona and Costantini, 2011). Moreover, several studies have demonstrated $PM_{2.5}$-associated inorganic and organic components are responsible for its toxic effects, all of them have described the

Abbreviations: EC, elemental carbon; DAPI, 4,6-diamido-2-phenylindole hydrochloride; DCF, 2′,7′-dichlorofluorescein; DCFH-DA, 2′,7′-dichlorodihydrofluorescein diacetate; LC3, microtubule-associated proteins light chain 3; LDH, lactate dehydrogenase; NAC, N-acetylcysteine; $O_2^{\cdot-}$, superoxide anion; OC, organic carbon; $OH^{\cdot}$, hydroxyl radical; PAHs, polycyclic aromatic hydrocarbons; PM, ambient airborne particulate matter; ROS, reactive oxygen species; SEM, scanning electron microscopy; TEM, transmission electron microscopy.

* Corresponding authors. Tel.: +86 10 84205133; fax: +86 10 64222965 (Z. Feng), tel.: +86 10 88256460; fax: +86 10 88256290 (W. Ding).

E-mail addresses: fengzhaohan@yahoo.com.cn (Z. Feng), dingwj@ucas.ac.cn (W. Ding).

0887-2333/$ - see front matter Crown Copyright © 2013 Published by Elsevier Ltd. All rights reserved.
http://dx.doi.org/10.1016/j.tiv.2013.05.004

oxidative stress as common pathway for $PM_{2.5}$-induced oxidative damage in A549 cells (Billet et al., 2007; Kouassi et al., 2010; Viola et al., 2011; Yi et al., 2012). Excessive levels of ROS, mainly radical form, can cause severe damage to DNA, RNA and proteins (Brigelius-Flohé, 2009). In this respect, subcellular degradation by autophagy may play an essential role in maintaining cell functionality.

Autophagy is the cellular pathway of a self-digestion process that regulates the degradation and recycling of unnecessary intracellular proteins and dysfunctional organelles (Azad et al., 2009; Abounit et al., 2012). During autophay, these cytoplasmic materials are sequestered into double-membraned vesicles (autophagosomes), which fuse with lysosomes to form autolysosomes, and further degrade by lysomal hydrolases (Abounit et al., 2012; Chen et al., 2007). The formation of the autophagosome is involved in various autophagy-related proteins, such as Atg5, Atg12, Beclin1, and microtubule-associated proteins light chain 3 (LC3) (Van Limbergen et al., 2009). Therefore, autophagy has been conventionally considered to be a pathway contributing to cellular homeostasis and adaptation to stress (White and DiPaola, 2009). It has been demonstrated that autophagy also functions as a cytoprotective response against various types of cellular stress by providing the cell with metabolic substrates (Chen et al., 2012). Recently, it was confirmed that ROS can trigger autophagy through several distinct mechanisms involving Atg4, catalase, and the mitochondrial electron transport chain (mETC) (Azad et al., 2009). Although the lung is a primary site of exposure for many inhaled chemical pollutants, the mechanisms underlying $PM_{2.5}$ related regulation of autophagy has not been fully elucidated.

This work aims to explore the mechanism of $PM_{2.5}$-related antioxidant defenses and autophagy by employing human lung epithelial A549 cells. Moreover, the function of ROS in this process is also investigated.

2. Materials and methods

2.1. Materials

A549 cells were obtained from the Cell Bank of Peking Union Medical College (Beijing, China). 3-(4,5-dimethylthiazol-2-yl)-2,5-diphenyltetrazolium bromide (methyl tetrazolium, oiMTT), dimethylsulfoxide (DMSO), 2′,7′-dichlorodihydrofluorescein diacetate (DCFH-DA) were purchased from Sigma (St. Louis, MO, USA). Anti-LC3 antibody was obtained from ProteinTech Biotechnology (ProteinTech Ltd. Wuhan, China). Lipofectamine 2000, TRIZOL and Dulbecco's modified Eagle's medium (DMEM) were obtained from Invitrogen (CA, USA). Fetal bovine serum was purchased from PAA (Linz, AUS). 24-well plates and cell culture dishes were obtained from Costar Cambridge (MA, USA). Phenylmethanesulfonyl fluoride (PMSF) was purchased from Ameresco (MA, USA). All other chemicals, including penicillin, streptomycin, RIPA buffer, rapamycin, protease inhibitors, 4,6-diamido-2-phenylindole dihydrochloride (DAPI) were obtained from Beyotime (Beijing, China). GFP-LC3 plasmid was kindly provided by Dr. M. Zheng (Nebraska Medical Center, Omaha, USA).

2.2. $PM_{2.5}$ sampling

$PM_{2.5}$ samples were collected at Yuquan Road, Beijing, China in January–June, 2009. The sampling site is approximately 8 km away from an iron and steel factory. $PM_{2.5}$ samples were collected on nitrocellulose filters (diameter = 47 mm, Pall Life Sciences, NY, USA) for biological assay or quartz filters for chemical characterization using a low volume samplers (about 24 L/min, Beijing Geology Device Company, Beijing, China) for 12 h (8:00–20:00). The quartz filters were preheated at 450 °C for 4 h before sampling, and all filters were equilibrated in a condition of 30% relative humidity and 25 °C room temperature for over 48 h and then weighted on a high-precision microbalance (Mettler Toledo, AG258, OH, USA) to measure atmospheric daily $PM_{2.5}$ concentration. All sampled filters were stored in the darkness at −20 °C before further chemical and physical characterization. Blanks (unexposed filters) were prepared using the same method as for the samples except for sampling, which were used as a control in all experiments.

$PM_{2.5}$ samples on nitrocellulose filters were prepared according to the method of Imrich et al. (2000). Briefly, $PM_{2.5}$ samples were extracted from sampled filter strips by immersing them in deionized water and sonicating for 30 min (KQ-700V, 700W). The extracted samples were then stored at −80 °C until cell exposure.

2.3. $PM_{2.5}$ physical and chemical characterization

Size distribution of $PM_{2.5}$ was measured by a scanning electron microscopy (SEM, JEOL JSM-6700F, Tokyo, Japan) as described by Billet et al. (2007). Prior to analysis, $PM_{2.5}$ was suspended in an *n*-hexane solution with a assistance of ultrasonic treatment, and the suspended particles was then filtered through a nucleopore filter to obtain well distribution and dispersed $PM_{2.5}$, without agglomerates. The filter was then carbon coated, and measured using automatic mode. The minimal observable size was 0.1 μm.

The size distribution of $PM_{2.5}$ in suspension was analyzed using Nano-Zetasizer (1000 HS, Malvern Instrument Ltd., UK) based on dynamic light scattering measurement technique. Before measurement, $PM_{2.5}$ was firstly suspended in serum free culture medium, and sonicated for 30 s at 40 W in a bath to disperse the $PM_{2.5}$ by using ultrasonic processor (VCX130, Sonics, USA). The particle Z-Average was reported.

Daily $PM_{2.5}$ samples were chemically analyzed for polycyclic aromatic hydrocarbons (PAHs), elemental and organic carbon (EC and OC) and inorganic elements by splitting the same filter into 3 aliquots.

Polycyclic aromatic hydrocarbons (PAHs) was measured by a thermal desorption at 300 °C coupled with cold trapping, and followed by gas chromatography–mass spectrometry (GC/MS) analyses (Model 6890N Aglient, CA, UAS) equipped with a 60 m HP-5MS column as described by Zhang et al. (2009). 18 PAHs were analyzed in the $PM_{2.5}$ smaples including acenaphthylene, acenaphthene, anthracene, benzo[a]anthracene, benzo[b]fluoranthene, benzo[k]fluoranthene, benzo[a]pyrene, benzo[e]pyrene, benzo[ghi]perylene, chrysene, coronene, dibenz[a,h]anthracene, fluoranthene, indeno[123-cd]pyrene; fluorene, naphthalene, phenanthrene, and pyrene.

Elemental and organic carbon (EC and OC) in $PM_{2.5}$ were measured on-filter using a thermal–optical analyzer (Sunset Laboratories, NC, USA) following the ACE-Asia base case protocol as described in the methods of Zhang et al. (2008). Inorganic elements were determined by acid digestion of collected $PM_{2.5}$, followed by measurement using inductively coupled plasma-mass spectrometry (ICP-MS, Elemental X7, Thermo, MA, USA), for concentrations of Mg, Mn, Fe, Ca, Ni, Ti, V, Cr, Cu, Zn, As and Pb.

2.4. Cell culture and $PM_{2.5}$ treatment

Human lung epithelial A549 cells were maintained in low glucose DMEM supplemented with 10% fetal bovine serum (FBS, Hyclone, GA, USA) in a 5% CO_2 atmosphere at 37 °C. All cell exposure experiments were performed at 80–90% of cell confluence with viability $\geqslant$90% determined by the trypan blue staining. Once the cell reached confluence, the culture medium was replaced with 0.5% serum-containing medium.

A549 cells (1×10^4 cells/ml) were first cultured in plates (Costar Cambridge, MA, USA) for 12 h, then the cells were treated with $PM_{2.5}$ at the final concentration of 25, 50, 100 or 200 μg/ml for 4, 12, 24 or 48 h, respectively, or treated with rapamycin (50 nM) for 48 h.

2.5. MTT assay

MTT assay was carried out to evaluate the cell viability after exposure to $PM_{2.5}$ according to the method of Mosmann (Mosmann, 1983). After the exposure, 20 μl of MTT (2.5 mg/ml in PBS) were added to each well and the cells were incubation for 2 h at 37 °C. Cells were then treated with 200 μl of DMSO and the absorbance was quantified at 492 nm by a microplate spectrophotometer (Thermo MK3, MA, USA). The viability of the treated cells was expressed as a percentage relative to untreated cells, which was assumed to be 100%.

2.6. LDH assay

In order to determine cellular toxicity of $PM_{2.5}$, the level of lactate dehydrogenase (LDH) released from A549 cells was measured. After 48 h exposure to $PM_{2.5}$, cell-free supernatant aliquots were separated cells in each experimental sample by centrifuge, and supernatants were transferred to clean flat-bottom plate for enzymatic analysis. LDH in the culture supernatants was measured using commercially available LDH cytotoxicity detection kitPLUS (Roche Applied Science, Mannheim, Germany). All samples were assayed in duplicates for LDH content by a microplate spectrophotometer (Thermo MK3, MA, USA).

2.7. ROS assay

The intracellular levels of reactive oxygen species (ROS) in A549 cells were measured using DCFH-DA, a cell permeable nonfluorescent molecular probes oxidized by ROS to fluorescent compound 2′,7′-dichlorofluorescein (DCF). DCFH-DA, dissolved in ethanol, was added to cell culture at a final concentration of 40 μM for 30 min. Cells were washed with PBS and then incubated with 25, 50, 100, or 200 μg/ml of $PM_{2.5}$ for 4, 12, 24 or 48 h at 37 °C, respectively. The cells were lysed with 200 mM of NaOH. The total green fluorescence intensity of each well was quantified using a fluorescence multi-well plate reader (TriStar LB 941, Berthold, Germany) with excitation and emission wavelengths of 485 nm and 530 nm, respectively. The total protein concentration was determined using bicinchoninic acid (BCA) protein assay kits (Pierce, IL, USA).

2.8. Antioxidant enzyme assays

The intracellular catalase (CAT) and superoxide dismutase (SOD) activities were determined by commercially available superoxide dismutase and catalase assay kits following the manufacturer's instruction (Beyotime, Beijing, China). After exposure of A549 cells to 25, 50, 100 or 200 μg/ml of $PM_{2.5}$ for 48 h, the cells were washed twice with cold PBS and then lysed with 50 mM Tris buffer containing 1% Triton X-100 and 100 μg/ml of protease inhibitors at *pH* 7.4. The supernatants for enzyme assays were separated by centrifuging at 10,000 *g* for 15 min. The CAT activity was quantified spectrophotometrically by measuring the decrease in (H_2O_2) absorbance at 240 nm in the presence of CAT. One unit of CAT was defined as 1 mM of H_2O_2 consumed per minute. The SOD activity was measured by the rate of oxidation of 5,6,6a,11b-tetrahydroxylbenzo[c]fluorene in aqueous alkaline solution to yield a chromophore that absorbs at 525 nm. One unit of SOD was velocity control compared to the ratio provided by the manufacturer. Results are reported as U/mg of protein. Data were represented as the fold of the CAT or SOD activity relative to untreated cells. The total protein concentration was measured as described above.

2.9. Observation of autophagosome

After exposure of A549 cells to 100 μg/ml of $PM_{2.5}$ for 48 h, the cells were fixed with 2.0% glutaraldehyde in 0.1 M cacodylate buffered (*pH* 7.4) at 4 °C overnight. After postfixation with 1% OsO_4 in 0.1 M sodium cacodylate buffer (*pH* 7.4) at 4 °C for 2 h, the cells were dehydrated with ascending concentrations of ethanol (50–100%), and embedded at 60 °C for 2 days. Ultrathin sections (80 nm) were stained with uranyl acetate and lead citrate. The sections were examined using transmission electron microscopy (TEM) (Model JEM-1400; JEOL, Tokyo, Japan) at 100 kV.

2.10. Real-time PCR analyses

After exposure to 0, 25, 50, 100, or 200 μg/ml of $PM_{2.5}$ for 48 h, total RNA of the A549 cells was extracted with TRIZOL according to the protocol of the manufacturer. The cDNA was used as a template to examine the mRNA expression levels of *atg5* and *beclin1* by using SYBR green supermix (Toyobo, ShangHai, China). The primer sequences for real-time PCR were as follows: *β-actin*, 5′-TGACGTGGACATCCGCAAAG-3' (sense), 5'-CTGGAAGGG-ACAGCGAGG-3′ (antisense); *atg5*, 5′-TCTGCTTTCCTCCACTGCCAT-3′ (sense), 5′-GGCCAAAGGTTTCAGCTTCATT-3′ (antisense); *beclin1*, 5′-GGCACAATCAATAACT-TCAGGC-3′ (sense), 5′-TTATTGGCCAGAGCATGGAG-3′ (anti-sense). The PCR cycle was as follows: initial denaturant at 95 °C for 5 min, followed by 40 cycles of denaturant at 95 °C for 30 s, annealing at 60 °C for 30 s and extension at 72 °C for 30 s. The amount of target genes was analyzed using the ΔCt method following the normalization through β-actin.

2.11. LC3 subcellular distribution

A549 cells were first cultured on polylysine-coated coverslip in a 24-well plate with 70% confluence, and then cotransfected with 0.8 μg of GFP-LC3 plasmid for 24 h using Lipofectamine 2000 according to the manufacturer's instructions. The transfected cells were exposed to 100 μg/ml of $PM_{2.5}$ for 48 h in the DMEM without FBS. Rapamycin (50 nM) and H_2O_2 (100 μM) have been used as the positive control for autophagy. At the end of exposure, the cells were fixed in 4% paraformaldehyde for 10 min at room temperature. Slides were washed with PBS for three times, followed by nuclear staining with DAPI. Slides were examined using a Zeiss inverted LSM710 confocal microscope at 40× objectives. The intensity of GFP-LC3 dots was measured using Zeiss confocal software.

2.12. Western blotting analysis

After exposure to $PM_{2.5}$, A549 cells were separated from the culture medium and lysed in RIPA buffer containing 50 mM Tris, 150 mM NaCl, 1% Triton X-100, 1% sodium deoxycholate, 0.1% SDS and 1 mM PMSF (*pH* 7.4). Expression of LC3 and β-actin in whole cell lysates were subjected to sodium dodecyl sulfate polyacrylaminde gel electrophoresis (SDS–PAGE). The gels were transferred to polyvinylidene difluoride (PVDF) membrane by semidry electrophoretic transfer at 20 V for 60 min. The PVDF membranes were then blocked in 5% nonfat milk at room temperature for 1 h, and incubated with the primary antibody (dilution 1:1000) in Tris/buffered saline/Tween-20 (TBST) containing 5% bovine serum albumin for overnight in 4 °C and then incubated with the secondary antibody (dilution 1:1000) at room temperature for 1 h. The membrane was washed with TBST three times for 5 min each.

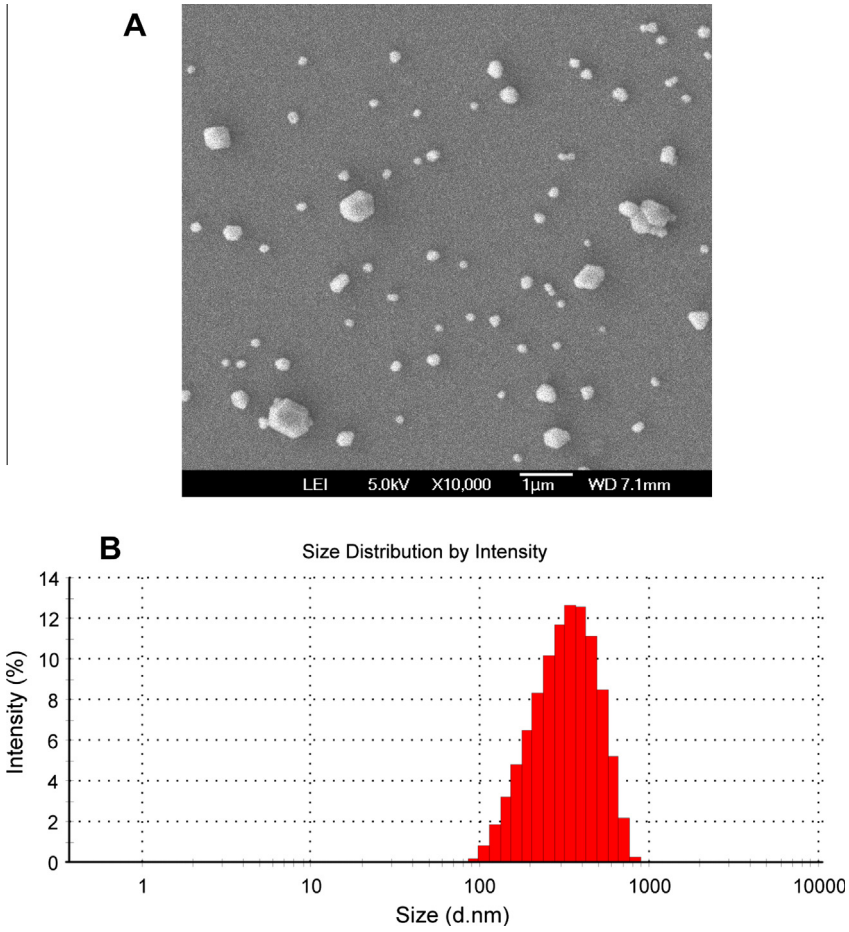

Fig. 1. $PM_{2.5}$ size distribution. (A) SEM image of $PM_{2.5}$ (Bar, 1 μm; magnification, 10,000×). (B) Particle size distribution in the DMEM medium was analyzed by dynamic light scattering.

Table 1
Organic compositions detected in $PM_{2.5}$.

PAHs	Concentration (ng/mg)
Acenaphthylene	22.99 ± 0.57
Acenaphthene	13.70 ± 0.55
Anthracene	5.67 ± 1.16
Benz[a]anthracene	157.40 ± 1.00
Benzo[b]fluoranthene	234.16 ± 21.83
Benzo[k]fluoranthene	84.93 ± 5.02
Benzo[a]pyrene	102.97 ± 8.11
Benzo[e]pyrene	92.40 ± 0.56
Benzo[ghi]perylene	90.94 ± 21.93
Chrysene	222.49 ± 7.09
Coronene	16.47 ± 5.58
Dibenz[a,h]anthracene	13.21 ± 2.64
Fluoranthene	228.44 ± 45.70
Fluorene	9.81 ± 0.74
Indeno[123-cd]pyrene	72.36 ± 8.11
Naphthalene	3.47 ± 0.52
Phenanthrene	196.63 ± 26.37
Pyrene	214.27 ± 41.32

Table 2
Carbon and metals detected in $PM_{2.5}$.

OC/EC	Concentration (μg/mg)
OC	458.3 ± 41.1
EC	9.04 ± 0.21
OC/EC	50.15 ± 5.18
Metals	**Concentration (ng/mg)**
Mg	4602 ± 24
Pb	285 ± 1
Ca	2126 ± 144
Ti	351 ± 1
V	38 ± 0.1
Cr	78 ± 1
Mn	641 ± 2
Fe	1736 ± 15
Ni	55 ± 1
Cu	342 ± 2
Zn	4659 ± 732
As	335 ± 0.4

β-actin was used as loading controls for the total protein content and showed no differences between groups.

2.13. Statistical analysis

All results obtained were expressed as means ± standard deviation (SD) of three independent experiments. Data were analyzed using two way analysis of variance (ANOVA) statistical analysis followed by a post hoc t test or one way analysis of variance (ANOVA) followed by post hoc comparisons using the Tukey's multiple paired comparison test. A probability of value of $p < 0.05$ was considered as statistically significant.

3. Results

3.1. $PM_{2.5}$ physical and chemical characteristics

The morphology of $PM_{2.5}$ particles by SEM showed a size range of 0.1–1 μm (Fig. 1A). A dynamic light scattering measurement revealed a size range of 0.09–1 μm with a mean of 0.43 μm (Fig. 1B).

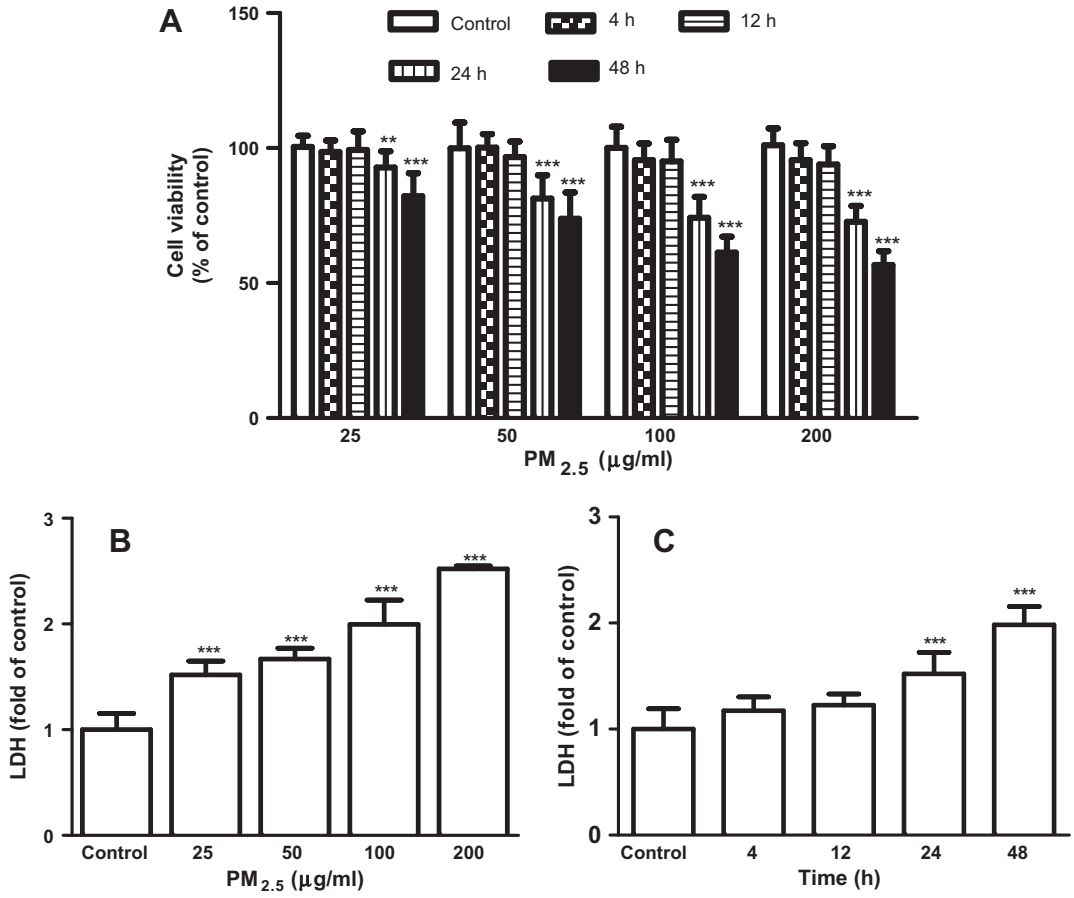

Fig. 2. Effect of $PM_{2.5}$ exposure on cell viability in A549 cells. (A) MTT assay. A549 cells were treated with 25, 50, 100 or 200 μg/ml of $PM_{2.5}$ for 4, 12, 24 or 48 h, respectively. After treatment, cell viability was determined by MTT assay. (B) LDH release. A549 cells were treated with 25, 50, 100 or 200 μg/ml of $PM_{2.5}$ for 48 h (B), or 100 μg/ml of $PM_{2.5}$ for 4, 12, 24 or 48 h (C). Data are means ± SD of three independent experiments. $^{**}p < 0.01$ and $^{***}p < 0.001$ vs. control.

The analytical results of PAHs (Table 1) showed that benzo[b]fluoranthene (234.16 ± 21.83 ng/mg), chrysene (222.49 ± 7.09 ng/mg), fluoranthene (228.44 ± 45.70 ng/mg), phenanthrene (196.63 ± 26.37 ng/mg) and pyrene (214.27 ± 41.32 ng/mg) were the dominant PAHs in the $PM_{2.5}$. The average concentrations of OC and EC in the $PM_{2.5}$ were 453.8 ± 41.1 μg/mg and 9.04 ± 0.21 μg/mg (Table 2), and the OC/EC ratio was about 50 ± 5.18. Among the total of 12 metal elements measured, Mg, Ca, Fe and Zn were the most abundant elements in the $PM_{2.5}$ (Table 2).

3.2. Cell viability and cytotoxicity induced by $PM_{2.5}$

The cell viability examined by MTT assay showed that compared with the unexposed control cells, no statistically significant impacts of $PM_{2.5}$ were detected after 12 h of exposure to 25, 50, 100 or 200 μg/ml of $PM_{2.5}$. However, a dose-dependent decrease of cell viability was observed after 24 and 48 h exposure (Fig. 2).

The level of LDH released from the $PM_{2.5}$-treated cells significantly increased after 48 h of exposure in a dose-dependent manner (Fig. 2B), and LDH levels were significantly increased after 24 and 48 h of exposure to 100 μg/ml of $PM_{2.5}$ compared with the unexposed control cells (Fig. 2C). The results indicate that the amount of LDH released from the cells induced by $PM_{2.5}$ is related to the cell viability.

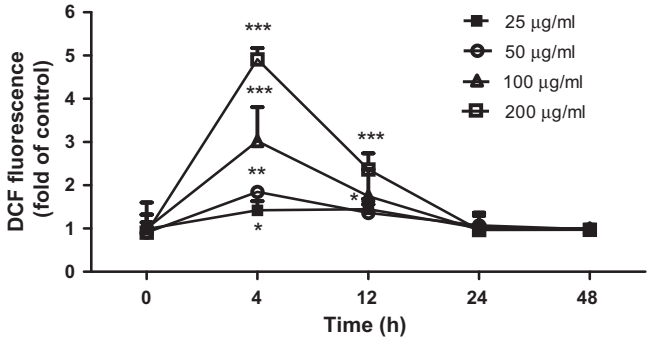

Fig. 3. Effect of $PM_{2.5}$ exposure on ROS generation in A549 cells. A549 cells were treated with the following $PM_{2.5}$ concentrations: 25 μg/ml (closed squares), 50 μg/ml (open round), 100 μg/ml (open triangle) and 200 μg/ml (open squares) for 4, 12, or 24 h. Intracellular levels of ROS were determined using DCFH-DA staining. The DCF fluorescence values were expressed as fluorescence ratio (fold) between the exposed cells and the unexposed control cells. Data are means ± SD of three independent experiments. $^{*}p < 0.05$, $^{**}p < 0.01$, $^{***}p < 0.001$ vs. control.

3.3. $PM_{2.5}$ induced ROS generation

By measuring the DCF fluorescence intensity in A549 cells after exposed to $PM_{2.5}$ at 25, 50, 100 or 200 μg/ml of $PM_{2.5}$ for 4, 12, 24 or 48 h, respectively. A dose-dependent increase of intracellular ROS generation was observed (Fig. 3), while the DCF fluorescence intensities reached peak values at 4 h of exposure and dropped to the base level after 24 h. At 4 and 12 h of exposure, the DCF

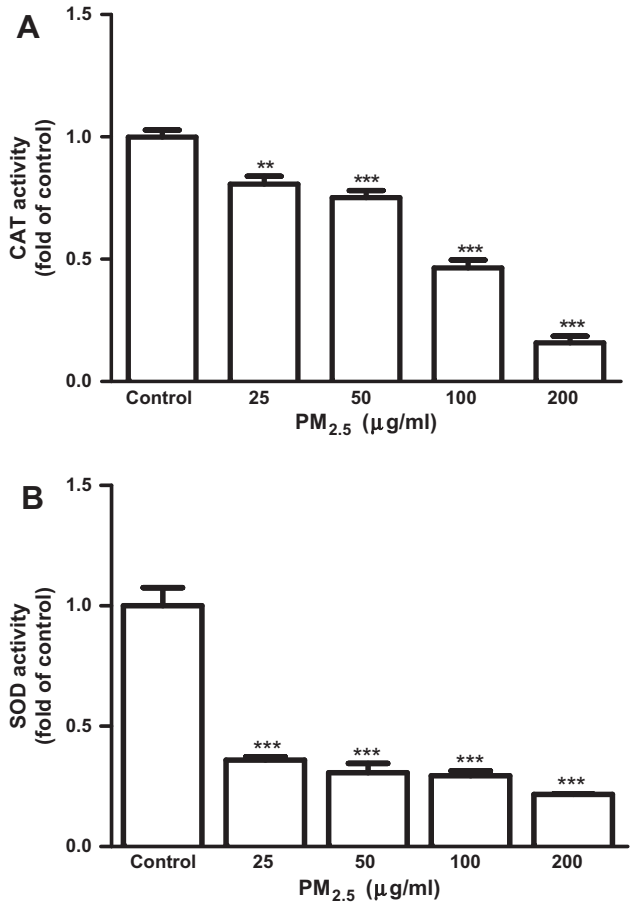

Fig. 4. Effect of $PM_{2.5}$ exposure on activity of antioxidant enzymes in A549 cells. A549 cells were treated for 48 h with $PM_{2.5}$ at the indicated concentrations. (A) Catalase (CAT), (B) Superoxide dismutase (SOD). Data are means ± SD of three independent experiments. $^{**}p < 0.01$ and $^{***}p < 0.001$ vs. control.

fluorescence intensities were significantly higher compared with the unexposed control cells (Fig. 3).

3.4. $PM_{2.5}$ impaired the antioxidant enzymatic defenses

As shown in Fig. 4, the activities of SOD and CAT in A549 cells were significantly decreased in a dose-dependent manner after exposure to $PM_{2.5}$ for 48 h, indicating $PM_{2.5}$ induced oxidative stress in the intracellular antioxidant enzymatic defenses.

3.5. $PM_{2.5}$ induced autophagy

Typical autophagosomes with double membranes and cellular contents were observed in the TEM images of A549 cells which have exposed to 100 μg/ml of $PM_{2.5}$ for 48 h (Fig. 5A (b)). Compared to the unexposed control cells (Fig. 5A (a)), many multivesicular and membrane-rich autophagosomes were in close proximity to each other (Fig. 5A (b)), indicating $PM_{2.5}$-induced autophagosome formation at the ultrastructural level of the exposed A549 cells.

Autophagosome formation by translocation of the autophagosome protein GFP-LC3 from the cytosol (diffuse distribution) to newly formed autophagosomes which appear as cytoplasmic puncta was monitored to establish the dynamics of autophagic processes (Chen et al., 2012). The results (Fig. 5B) showed when the transfected A549 cells were exposed to 100 μg/ml of $PM_{2.5}$ for 24 or 48 h or 50 nM of rapamycin and 100 μM of H_2O_2 for 48 h, respectively. GFP-LC3 as cytosolic LC3 was diffuse in the unexposed cells, while punctate patterns of fluorescent signals from GFP-LC3 similar to these induced by a positive control, rapamycin and H_2O_2, were readily observed in the $PM_{2.5}$ exposed cells as shown in the middle and right columns of Fig. 5B, indicating that $PM_{2.5}$ exposure induced both the initiation and maturation of autophagosomes after 24–48 h exposure.

LC3 has two species, an unprocessed 18 kDa cytosolic protein (LC3-I) and a processed 16 kDa protein (LC3-II) which is membrane-bound and increases during autophagy by conversion from LC3-I (Kondo and Kondo, 2006). A549 cells were exposed to 25, 50, 100 or 200 μg/ml of $PM_{2.5}$ for 48 h or 100 μg/ml of $PM_{2.5}$ for 12, 24 or 48 h, LC3-I and LC3-II levels in the exposed cells were measured, the western blotting results (Fig. 5C) showed that ratios of LC3-II to LC3-I content increase with the concentration of $PM_{2.5}$ and the exposure time, indicating $PM_{2.5}$ exposure induced conversion of LC3-I to LC3-II. Moreover, it was also observed that $PM_{2.5}$ significantly up-regulated the mRNA expressions of *atg5* and *beclin1* as another autophagy markers compared with the unexposed control cells, which is consistent with the quantification data of rapamycin (Fig. 5D). These results confirmed that $PM_{2.5}$ can induce autophagy in human A549 cells.

4. Discussion

Epidemiological evidences have demonstrated that the greatest health risk of PM is correlated with smaller PM (Levy et al., 2000). PM used in this work was smaller than 2.5 μm, which are respirable and able to penetrate to the alveolar region of the lung to exert their toxicity (Harrison and Yin, 2000).

PM toxicity is mainly related its composition (Harrison and Yin, 2000), including both organic and inorganic compounds (Gualtieri et al., 2010; Yi et al., 2012). Among detected 18 PAHs, relatively high concentrations of benzo[b]fluoranthene, fluoranthene, chrysene, pyrene, and phenanthrene were observed in the $PM_{2.5}$ samples, suggesting a significant contribution from anthropogenic source. OC and EC in PM play important roles in health, visibility and climate effects (Cao et al., 2005). OC/EC ratios can provide information on the origins of carbonaceous $PM_{2.5}$ (Chow et al., 1996). High concentrations of OC and EC were detected in the $PM_{2.5}$ samples, and the measured OC/EC ratio (50.15) is much higher than the reported values 12.0 in $PM_{2.5}$ originated from coal-combustion (Cao et al., 2005). This may reflect its multi-sources of coal combustion, motor-vehicle exhaust, and biomass burning sources in Beijing. Among 12 detected inorganic elements including natural sourced elements (Ca, Mg, Ti, etc.) and conventionally anthropogenic inorganic elements (Fe, Mn, Ni, Cr, Pb, Zn, Cu, etc.), the high levels of Mg, Ca, Fe and Zn were observed in the collected $PM_{2.5}$ samples, indicating its both natural and anthropogenic sources. All these results arising from the chemical characterization of collected $PM_{2.5}$ samples indicated that the $PM_{2.5}$ samples are a complex mixture of chemicals, and highly anthropogenic contribution.

Cell viability assays are vital steps in determining the cellular response to a toxicant, which give information on cell death, survival and metabolic activities (Lee et al., 2011). Particles are thought to impact on genotoxicity and cytotoxicity as well as cell proliferation (Knaapen et al., 2004). This work shows that LDH released from the cells exposed to $PM_{2.5}$ increases with the concentrations of $PM_{2.5}$ and the exposure time, indicating that the exposure of cells to the $PM_{2.5}$ decrease the cell viability (Fig. 2). It has been reported that particles from gasoline engine exhaust decrease cell viability in A549 cells (Zhang et al., 2007), and LDH level in rat alveolar macrophages is markedly increased in a dose-dependent manner by particle suspensions and water-soluble components of $PM_{2.5}$ (Geng et al., 2006), our observations are in agreement with these reports.

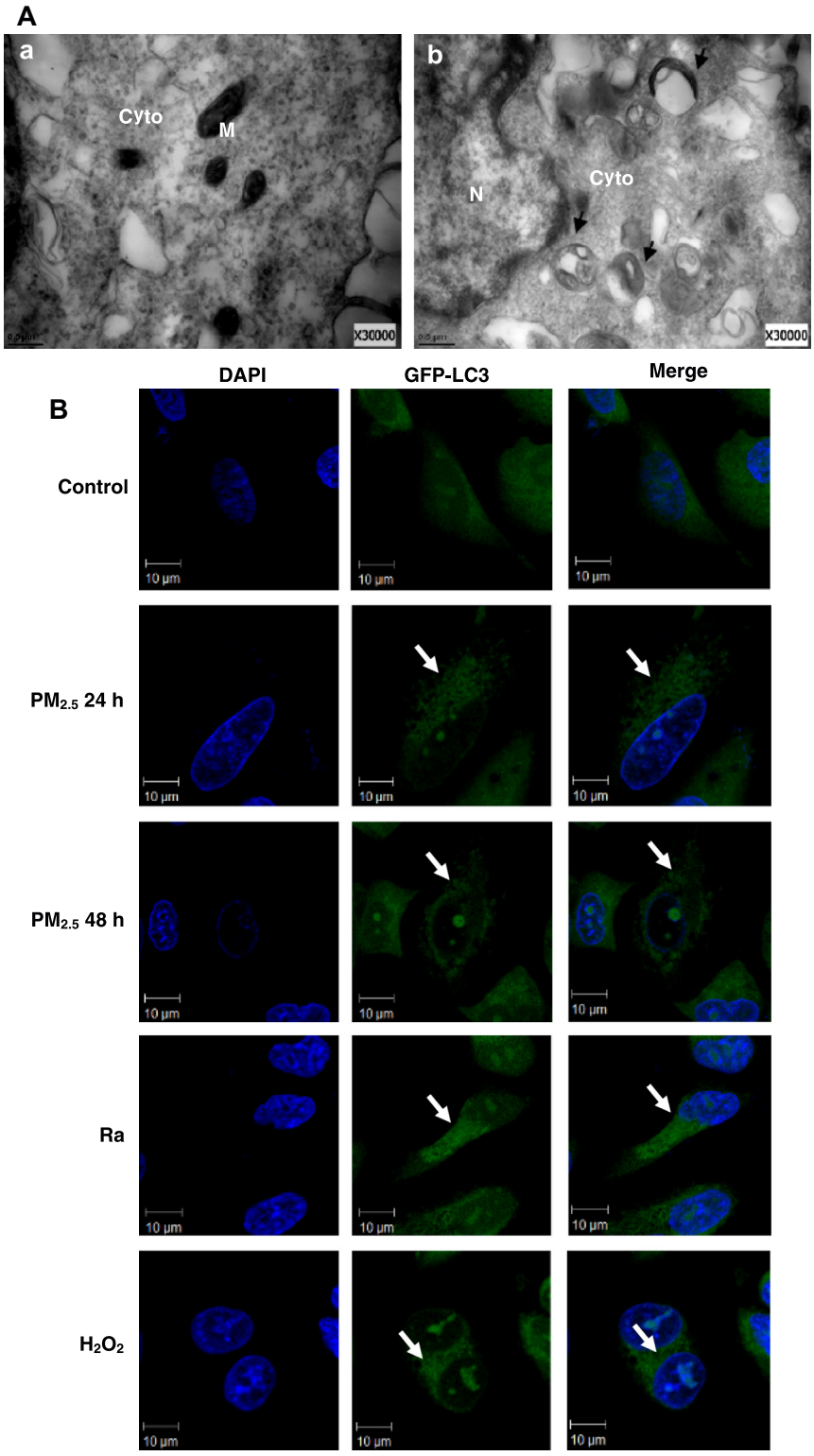

Fig. 5. Effect of $PM_{2.5}$ exposure on autophagy in A549 cells. (A) TEM images of autophagosomes in A549 cells. (a) Control cells. (b) Cells exposed to 100 μg/ml of $PM_{2.5}$ for 48 h. Black arrows indicate autophagosomes. Cyto means cytoplasm. N means nucleus. M means mitochondrial (Bar, 0.5 μm; magnification, 30,000×). (B) Confocal microscopy images of A549 cells. Cells were incubated with PBS, 100 μg/ml of $PM_{2.5}$ for 24 h and 48 h, or 100 μg/ml rapamycin and 100 μM H_2O_2 for 48 h (positive control for induction of autophagy), respectively. Autophagosome formations in A549 cells were detected by confocal microscopy. Scale bars as indicated in figure. White arrows indicate autophagosomes. Ra means rapamycin. (C) LC3-II accumulation in A549 cells. Cell lysates obtained upon exposure to $PM_{2.5}$ were used to perform Western blot experiments and evaluate protein expression. β-actin was used as the loading control. (D) The mRNA expression of autophagy-related genes. Cell lysates were used to perform real-time PCR experiments and evaluate the mRNA expression levels of *atg5*, and *beclin1* after 48 h of exposure to $PM_{2.5}$. Data are means ± SD of three independent experiments. $^{***}p < 0.001$ vs. control.

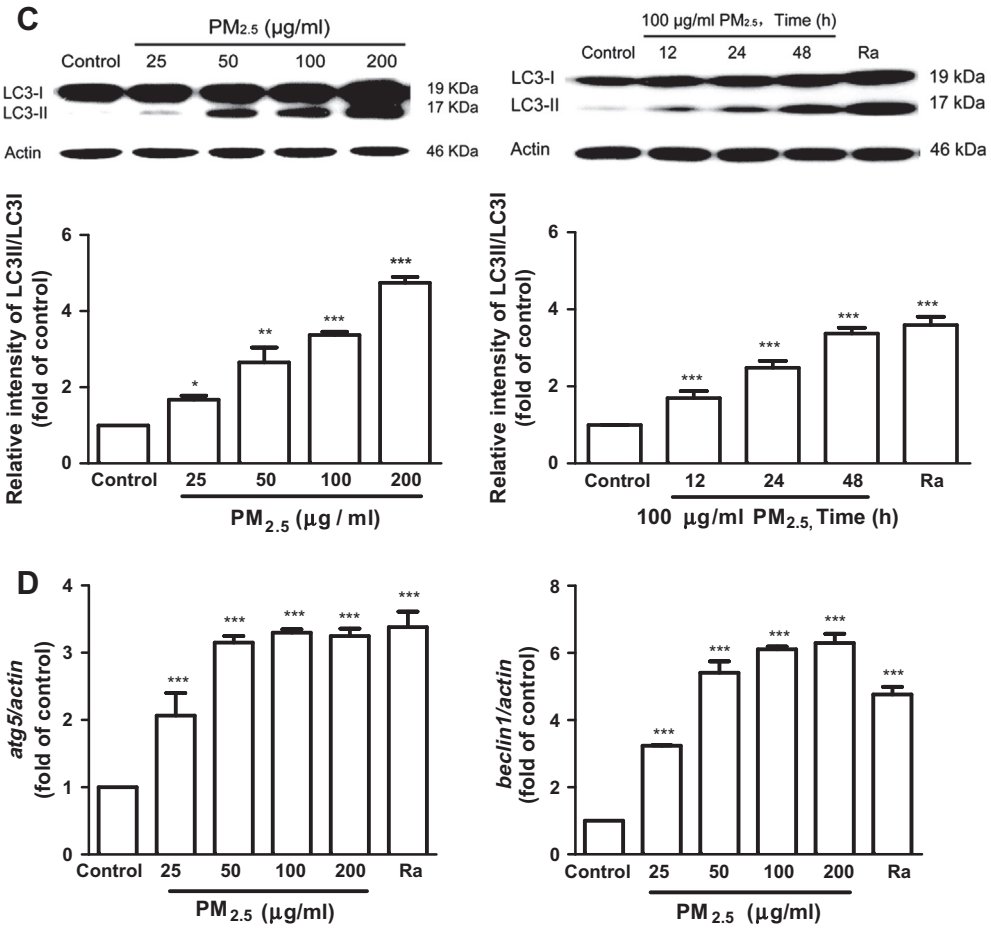

Fig. 5 (*continued*)

It has been reported that the oxidative stress as common pathway for $PM_{2.5}$-induced oxidative damage (Kouassi et al., 2010; Riva et al., 2011; Wei et al., 2011). It is difficult to determine the contribution of each contaminant in the $PM_{2.5}$ to the total oxidative stress, a number of investigations have demonstrated that metals, carbonaceous materials and PAHs can induce ROS formation (Billet et al., 2007; Cao et al., 2005; Geng et al., 2006; Ghio et al., 2012; Gualtieri et al., 2010, 2012; Yi et al., 2012). The high concentrations of PAHs, OC and EC, and transition metals observed in the collected $PM_{2.5}$ should contribute to the increase in intracellular ROS generation in the exposed A549 cells. It has also been reported that the cytotoxicity and oxidative stress, exerted by the $PM_{2.5}$, derived also from its oxidative potential, probably associated with particle-adsorbed transition metals and PAHs (Gualtieri et al., 2009).

Oxidative stress refers to an imbalance between excessive oxidant and antioxidant defenses that remove ROS (Leeuwenburgh and Heinecke, 2001). The antioxidant defenses including antioxidants (e.g. GSH) and antioxidant enzymes (e.g. SOD, GPx and CAT), prevent the generation of the most reactive form of ROS, i.e., $OH^{\cdot}$, and subsequent oxidative damage to various cell constituents, such as DNAs, proteins and lipids (Fridovich, 1986; Leeuwenburgh and Heinecke, 2001). SOD catalyzes the dismutation of $O_2^{\cdot}$ to H_2O_2, and CAT protects cells from removal of H_2O_2 (Koh and Kim, 2001). Our results showed that $PM_{2.5}$ induced loss of antioxidant enzymatic activities of SOD and CAT decease with the increased concentrations of $PM_{2.5}$ after 48 h of exposure (Fig. 4), this is in agreement with the report that PM_{10} impaired the antioxidant enzymatic activity of SOD, GR, CAT and glutathione-S-transferase in A549 cells (Chirino et al., 2010).

Autophagy may protect cells against cell deaths under oxidative stress, due to higher susceptibility of the oxidized proteins to be taken up by autophagosome, subsequently degraded by lysosome, which contributes to the efficient removal of oxidized proteins and reduce the further oxidative damage by these oxidants (Kiffin et al., 2006). Oxidant stress has been implicated to trigger autophagy by certain reagents such as hydrogen peroxide (H_2O_2) and 2-methoxyestradiol (2-ME) (Chen et al., 2007). This work showed that an evident increase in cytoplasmic vacuoles in cells exposed to $PM_{2.5}$ exposure, along with the formation of LC3 puncta and accumulation of LC3-II, which is the only protein marker that is reliably associated with completed autophagosomes. The analytic results of Western blotting showed an increase conversion of LC3-I to LC3-II in A549 cells exposed to $PM_{2.5}$ for 48 h. With the correlation between the amount of LC3-II and the extent of autophagosome formation, these results indicate that $PM_{2.5}$ toxic effects include triggering of autophagy in lung cells in culture. In addition, $PM_{2.5}$ exposure significantly increased the mRNA expression levels of autophagy-related protein Atg5 and Beclin 1, suggesting that Atg5 and Beclin 1 are also play roles in $PM_{2.5}$-induced autophagy (Kiyono et al., 2009). Thus, it can be concluded that exposure to $PM_{2.5}$ induces autophagy in A549 cells.

In summary, we have found that $PM_{2.5}$ can elicit oxidative stress by probably inducing ROS generation and causing loss of antioxidant enzymatic activity, resulting in accumulation of intracellular ROS and cell death in human epithelial lung A549 cells. The results suggest that $PM_{2.5}$-induced oxidative stress probably plays a key role in autophagy in A549 cells, which may contribute to $PM_{2.5}$-induced impairment of pulmonary function.

Conflict of interest

The authors declare that there is no conflict of interest.

Acknowledgements

This work was financially supported by grants from Gong-Yi Program of China Ministry of Environmental Protection (No. 200909016), National Natural Science Foundation of China (No. 10875170), the National Science and Technology Ministry of China (No. 2007BAC27B02-2), and Research Supported by the CAS/SAFEA International Partnership Program for Creative Research Teams. We thank Dr. Yuanxun Zhang and Dr. Junji Cao for valuable technical assistance and discussion.

References

Abounit, K., Scarabelli, T.M., McCauley, R.B., 2012. Autophagy in mammalian cells. World Journal of Biological Chemistry 3, 1–6.

Anderson, J.O., Thundiyil, J.G., Stolbach, A., 2012. Clearing the air: a review of the effects of particulate matter air pollution on human health. Journal of Medical Toxicology 8, 166–175.

Azad, M.B., Chen, Y., Gibson, S.B., 2009. Regulation of autophagy by reactive oxygen species (ROS): implications for cancer progression and treatment. Antioxidants & Redox Signaling 11, 777–790.

Billet, S., Garçon, G., Dagher, Z., Verdin, A., Ledoux, F., Cazier, F., Courcot, D., Aboukais, A., Shirali, P., 2007. Ambient particulate matter ($PM_{2.5}$): physicochemical characterization and metabolic activation of the organic fraction in human lung epithelial cells (A549). Environmental Research 105, 212–223.

Brigelius-Flohé, R., 2009. Commentary: oxidative stress reconsidered. Genes & Nutrition 4, 161–163.

Brunekreef, B., Holgate, S.T., 2002. Air pollution and health. Lancet 360, 1233–1242.

Cao, J., Chow, J.C., Lee, S., Li, Y., Chen, S., An, Z., Fung, K., Watson, J., Zhu, C., Liu, S., 2005. Characterization and source apportionment of atmospheric organic and elemental carbon during fall and winter of 2003 in Xi'an, China. Atmospheric Chemistry and Physics Discussions 5, 3561–3593.

Chen, Y., McMillan-Ward, E., Kong, J., Israels, S., Gibson, S., 2007. Oxidative stress induces autophagic cell death independent of apoptosis in transformed and cancer cells. Cell Death & Differentiation 15, 171–182.

Chen, L.H., Chu, P.M., Lee, Y.J., Tu, P.H., Chi, C.W., Lee, H.C., Chiou, S.H., 2012. Targeting protective autophagy exacerbates UV-triggered apoptotic cell death. International Journal of Molecular Sciences 13, 1209–1224.

Chirino, Y.I., Sánchez-Pérez, Y., Osornio-Vargas, Á.R., Morales-Bárcenas, R., Gutiérrez -Ruíz, M.C., Segura-García, Y., Rosas, I., Pedraza-Chaverri, J., García-Cuellar, C.M., 2010. PM_{10} impairs the antioxidant defense system and exacerbates oxidative stress driven cell death. Toxicology Letters 193, 209–216.

Chow, J.C., Watson, J.G., Lu, Z., Lowenthal, D.H., Frazier, C.A., Solomon, P.A., Thuillier, R.H., Magliano, K., 1996. Descriptive analysis of $PM_{2.5}$ and PM_{10} at regionally representative locations during SJVAQS/AUSPEX. Atmospheric Environment 30, 2079–2112.

Fridovich, I., 1986. Biological effects of the superoxide radical. Archives of Biochemistry and Biophysics 247, 1–11.

Geng, H., Meng, Z., Zhang, Q., 2006. In vitro responses of rat alveolar macrophages to particle suspensions and water-soluble components of dust storm $PM_{2.5}$. Toxicology in Vitro 20, 575–584.

Ghio, A.J., Carraway, M.S., Madden, M.C., 2012. Composition of air pollution particles and oxidative stress in cells, tissues, and living systems. Journal of Toxicology and Environmental Health, Part B 15, 1–21.

Gualtieri, M., Mantecca, P., Corvaja, V., Longhin, E., Perrone, M.G., Bolzacchini, E., Camatini, M., 2009. Winter fine particulate matter from Milan induces morphological and functional alterations in human pulmonary epithelial cells (A549). Toxicology Letters 188, 52–62.

Gualtieri, M., Øvrevik, J., Holme, J.A., Perrone, M.G., Bolzacchini, E., Schwarze, P.E., Camatini, M., 2010. Differences in cytotoxicity versus pro-inflammatory potency of different PM fractions in human epithelial lung cells. Toxicology in Vitro 24, 29–39.

Gualtieri, M., Longhin, E., Mattioli, M., Mantecca, P., Tinaglia, V., Mangano, E., Proverbio, M.C., Bestetti, G., Camatini, M., Battaglia, C., 2012. Gene expression profiling of A549 cells exposed to Milan $PM_{2.5}$. Toxicology Letters 209, 136–145.

Harrison, R.M., Yin, J., 2000. Particulate matter in the atmosphere: which particle properties are important for its effects on health? Science of the Total Environment 249, 85–101.

Imrich, A., Ning, Y.Y., Kobzik, L., 2000. Insoluble components of concentrated air particles mediate alveolar macrophage responses in vitro. Toxicology and Applied Pharmacology 167, 140–150.

Kiffin, R., Bandyopadhyay, U., Cuervo, A.M., 2006. Oxidative stress and autophagy. Antioxidants & Redox Signaling 8, 152–162.

Kiyono, K., Suzuki, H.I., Matsuyama, H., Morishita, Y., Komuro, A., Kano, M.R., Sugimoto, K., Miyazono, K., 2009. Autophagy is activated by TGF-β and potentiates TGF-β-mediated growth inhibition in human hepatocellular carcinoma cells. Cancer Research 69, 8844–8852.

Knaapen, A.M., Borm, P.J.A., Albrecht, C., Schins, R.P.F., 2004. Inhaled particles and lung cancer. Part A: Mechanisms. International Journal of Cancer 109, 799–809.

Koh, M., Kim, H.J., 2001. The effects of metallothionein on the activity of enzymes involved in removal of reactive oxygen species. Bulletin-Korean Chemical Society 22, 362–366.

Kondo, Y., Kondo, S., 2006. Autophagy and cancer therapy. Autophagy 2, 85–90.

Kouassi, K.S., Billet, S., Garcon, G., Verdin, A., Diouf, A., Cazier, F., Djaman, J., Courcot, D., Shirali, P., 2010. Oxidative damage induced in A549 cells by physically and chemically characterized air particulate matter ($PM_{2.5}$) collected in Abidjan, Côte d'Ivoire. Journal of Applied Toxicology 30, 310–320.

Lee, Y.S., Kim, D.W., Lee, Y.H., Oh, J.H., Yoon, S., Choi, M.S., Lee, S.K., Kim, J.W., Lee, K., Song, C.W., 2011. Silver nanoparticles induce apoptosis and G2/M arrest via PKCζ-dependent signaling in A549 lung cells. Archives of Toxicology 85, 1529–1540.

Leeuwenburgh, C., Heinecke, J., 2001. Oxidative stress and antioxidants in exercise. Current Medicinal Chemistry 8, 829–838.

Levy, J.I., Hammitt, J.K., Spengler, J.D., 2000. Estimating the mortality impacts of particulate matter: what can be learned from between-study variability? Environmental Health Perspectives 108, 109–117.

Mosmann, T., 1983. Rapid colorimetric assay for cellular growth and survival: application to proliferation and cytotoxicity assays. Journal of Immunological Methods 65, 55–63.

Pamplona, R., Costantini, D., 2011. Molecular and structural antioxidant defenses against oxidative stress in animals. American Journal of Physiology-Regulatory, Integrative and Comparative Physiology 301, R843–863.

Pope III, C.A., Burnett, R.T., Thun, M.J., Calle, E.E., Krewski, D., Ito, K., Thurston, G.D., 2002. Lung cancer, cardiopulmonary mortality, and long-term exposure to fine particulate air pollution. JAMA: the Journal of the American Medical Association 287, 1132–1141.

Riva, D., Magalhaes, C., Lopes, A., Lancas, T., Mauad, T., Malm, O., Valenca, S., Saldiva, P., Faffe, D., Zin, W., 2011. Low dose of fine particulate matter ($PM_{2.5}$) can induce acute oxidative stress, inflammation and pulmonary impairment in healthy mice. Inhalation Toxicology 23, 257–267.

Van Limbergen, J., Stevens, C., Nimmo, E., Wilson, D., Satsangi, J., 2009. Autophagy: from basic science to clinical application. Mucosal Immunology 2, 315–330.

Viola, G., Bortolozzi, R., Hamel, E., Moro, S., Brun, P., Castagliuolo, I., Ferlin, M.G., Basso, G., 2011. MG-2477, a new tubulin inhibitor, induces autophagy through inhibition of the Akt/mTOR pathway and delayed apoptosis in A549 cells. Biochemical Pharmacology 83, 16–26.

Wei, H., Wei, D., Yi, S., Zhang, F., Ding, W., 2011. Oxidative stress induced by urban fine particles in cultured EA. hy926 cells. Human & Experimental Toxicology 30, 579–590.

White, E., DiPaola, R.S., 2009. The double-edged sword of autophagy modulation in cancer. Clinical Cancer Research 15, 5308–5316.

Wu, W.-S., 2006. The signaling mechanism of ROS in tumor progression. Cancer and Metastasis Reviews 25, 695–705.

Yi, S., Zhang, F., Qu, F., Ding, W., 2012. Water-insoluble fraction of airborne particulate matter (PM_{10}) induces oxidative stress in human lung epithelial A549 cells. Environmental Toxicology. http://dx.doi.org/10.1002/tox.21750.

Zhang, Z.Z., Che, W.J., Liang, Y., Wu, M., Li, N., Shu, Y., Liu, F., Wu, D.S., 2007. Comparison of cytotoxicity and genotoxicity induced by the extracts of methanol and gasoline engine exhausts. Toxicology in Vitro 21, 1058–1065.

Zhang, Y., Schauer, J.J., Zeng, L., Wei, Y., Liu, Y., Shao, M., 2008. Characteristics of particulate carbon emissions from real-world Chinese coal combustion. Environmental Science & Technology 42, 5068–5073.

Zhang, Y.X., Schauer, J.J., Stone, E.A., Zhang, Y., Shao, M., Wei, Y., Zhu, X., 2009. Harmonizing molecular marker analyses of organic aerosols. Aerosol Science and Technology 43, 275–283.